

*Carnegie Observatories Astrophysics Series, Vol. 1:
Coevolution of Black Holes and Galaxies
ed. L. C. Ho (Cambridge: Cambridge Univ. Press)*

Black Holes in Active Galaxies

AARON J. BARTH
California Institute of Technology

Abstract

Recent years have seen tremendous progress in the quest to detect supermassive black holes in the centers of nearby galaxies, and gas-dynamical measurements of the central masses of active galaxies have been valuable contributions to the local black hole census. This review summarizes measurement techniques and results from observations of spatially resolved gas disks in active galaxies, and reverberation mapping of the broad-line regions of Seyfert galaxies and quasars. Future prospects for the study of black hole masses in active galaxies, both locally and at high redshift, are discussed.

1.1 Introduction

The detection of supermassive black holes in the nuclei of many nearby galaxies has been one of the most exciting discoveries in extragalactic astronomy during the past decade. Accretion onto black holes has long been understood as the best explanation for the enormous luminosities of quasars (Salpeter 1964; Zel'dovich & Novikov 1964; Rees 1984), and the luminosity generated by quasars over the history of the Universe implies that most large galaxies must contain a black hole as a relic of an earlier quasar phase (Softan 1982; Chokshi & Turner 1992; Small & Blandford 1992). While the search for evidence of black holes in nearby galaxies began 25 years ago with the seminal studies of M87 by Sargent et al. (1978) and Young et al. (1978), only a handful of galaxies were accessible to such measurements until the repair of the *Hubble Space Telescope (HST)* in 1993 made it possible to study the central dynamics of galaxies routinely at $0''.1$ resolution. In addition to the recent dynamical searches for black holes in active and inactive galaxies with *HST*, the existence of black holes has been further confirmed by ground-based observations of the Galactic Center (see Ghez, this volume) and by radio observations of the H_2O maser disk in the Seyfert 2 galaxy NGC 4258 (Miyoshi et al. 1995). As the evidence for supermassive black holes in galaxy centers has strengthened, it has become clear that nuclear activity and the growth of black holes must be integral components of the galaxy formation process.

With measurements of black hole masses in several galaxies, it became possible for the first time to study the demographics of the black hole population and the connection of the black holes with their host galaxies. Kormendy & Richstone (1995) showed that M_\bullet was correlated with L_{bulge} , the luminosity of the spheroidal “bulge” component of the host galaxy, albeit with substantial scatter. More intriguing was the discovery that M_\bullet is very tightly

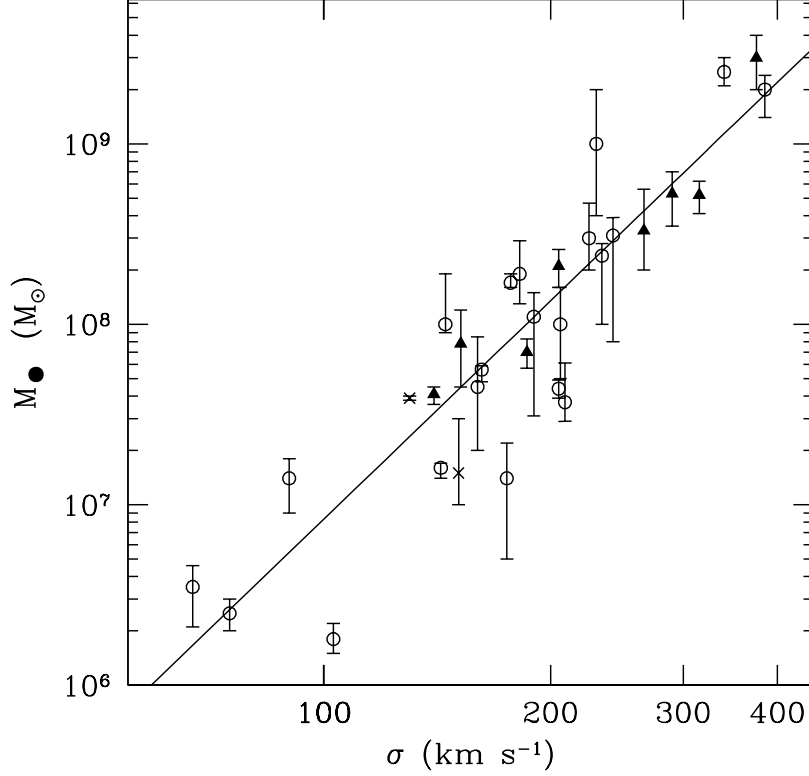


Fig. 1.1. The correlation between black hole mass and stellar velocity dispersion. Triangles denote galaxies measured with *HST* observations of gas dynamics, crosses are H_2O maser galaxies, and circles denote stellar-dynamical detections. The diagonal line is the best fit to the data as determined by Tremaine et al. (2002).

correlated with σ_* , the stellar velocity dispersion in the host galaxy (Ferrarese & Merritt 2000; Gebhardt et al. 2000a). The scatter in this relation is surprisingly small; Tremaine et al. (2002) estimate the dispersion to be < 0.3 dex in $\log M_\bullet$ at a given value of σ_* . This is a remarkable finding: it implies that the masses of black holes, objects that inhabit scales of $\lesssim 10^{-4}$ pc in galaxy nuclei, are almost *completely* determined by the bulk properties of their host galaxies on scales of hundreds or thousands of parsecs. Although the $M_\bullet - \sigma_*$ correlation is well established, its slope, and the amount of intrinsic scatter, remain somewhat controversial. The currently available sample of galaxies with accurate determinations of M_\bullet is still modest. More measurements of black hole masses in nearby galaxies are needed, over the widest possible range of host galaxy types and velocity dispersions, in order to obtain a definitive present-day black hole census.

Gas-dynamical measurements of black hole masses in active galactic nuclei (AGNs) are an essential contribution to this pursuit, as illustrated in Figure 1.1. *HST* observations of ionized gas disks are vitally important for tracing the upper end of the black hole mass

function, where stellar-dynamical measurements are hampered both by the low stellar surface brightness of the most massive elliptical galaxies and by the possibility of velocity anisotropy in nonrotating ellipticals. Observations of maser emission from molecular disks in active galaxies have provided the most solid black hole detection outside of our own Galaxy, strengthening the case that the massive dark objects discovered in *HST* surveys are indeed likely to be supermassive black holes. Reverberation mapping, and secondary methods that are calibrated by comparison with the reverberation technique, offer the most promising methods to determine black hole masses at high redshift.

The topic of black holes in active galaxies is vast, and this review will only concentrate on gas-dynamical measurements of black hole masses in AGNs. Before discussing the methods and results, a few general comments are in order. As Kormendy & Richstone (1995) have pointed out, there is a potentially serious drawback to any measurement technique based on gas dynamics: unlike stars, gas can respond to nongravitational forces, and the motions of gas clouds do not always reflect the underlying gravitational potential. For all methods based on gas dynamics, it is absolutely crucial to verify that the gas is actually in gravitational orbits about the central mass. If, for example, AGN-driven outflows or other nongravitational motions dominate, then black hole masses derived under the assumption of gravitational dynamics will be seriously compromised or completely erroneous. With that said, there are now numerous examples of ionized gas disks, and at least one maser disk, that clearly show orderly circular rotation. For reverberation mapping, the dynamical state of the broad-line emitting gas is more difficult to ascertain, but as discussed in §1.4 below, recent observations have provided some encouragement.

It must also be emphasized that, while these measurement techniques are capable of detecting dark mass concentrations in the centers of galaxies and determining their masses with varying degrees of accuracy, the observations do not actually prove that the dark mass is in the form of a supermassive black hole. The spatial resolution of gas-dynamical observations with *HST* typically corresponds to $\sim 10^{5-6}$ Schwarzschild radii. This is often sufficient to resolve the region over which the black hole dominates the gravitational potential of its host galaxy, but optical techniques are incapable of resolving the region in which relativistic motion occurs in the strong gravitational field near the black hole's event horizon. The conclusion that the massive dark objects detected in nearby galaxies are actually black holes is supported by the two most convincing dynamical detections, in our own Galaxy and in NGC 4258; in both objects the density of the central dark mass is inferred to be so large that reasonable alternatives to a black hole can be ruled out (Maoz 1998; Ghez, this volume). The best evidence for highly relativistic motion in the inner accretion disks of AGNs comes from X-ray spectra showing extremely broadened ($\sim 0.3c$), gravitationally redshifted Fe K line emission in Seyfert nuclei (Tanaka et al. 1995; Nandra et al. 1997). While this signature has only been convincingly detected in a handful of objects, it offers a powerful confirmation of the AGN paradigm, and analysis of the relativistically broadened line profiles may even reveal evidence for the black hole's spin (e.g., Iwasawa et al. 1996).

1.2 Black Hole Masses from Dynamics of Ionized Gas Disks

A striking discovery from the first years of *HST* observations was the presence of round, flattened disks of ionized gas and dust in the centers of some nearby radio galaxies (Jaffe et al. 1993; Ford et al. 1994). It was previously known from ground-based imaging that many ellipticals contained nuclear patches of dust (Kotanyi & Ekers 1979; Sadler &

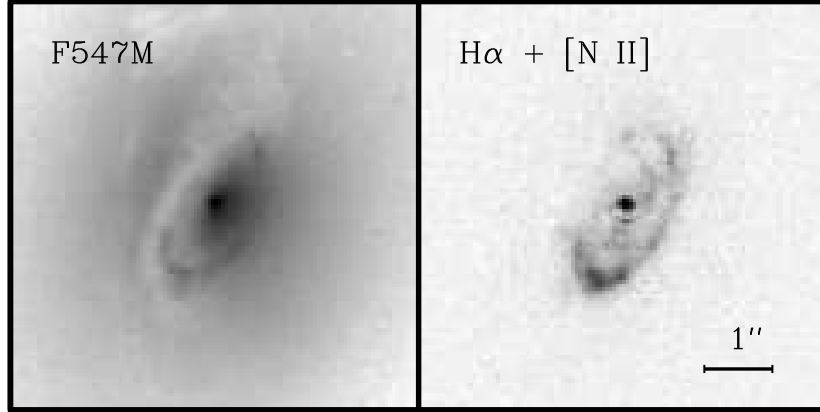


Fig. 1.2. An example of a dusty emission-line disk: *HST* images of the S0 galaxy NGC 3245. The left panel is a continuum image taken with the *HST* F547M filter (equivalent to the *V* band), and the right panel shows a continuum-subtracted, narrow-band image isolating the $H\alpha$ and $[N II]$ emission lines. At $D = 21$ Mpc, $1''$ corresponds to 100 pc.

Gerhard 1985; Ebner, Davis, & Djorgovski 1988), but *HST* revealed that the dust was often arranged in well-defined disks too small to be resolved from the ground. Imaging surveys with *HST* have found such disks, with typical radii of 100–1000 pc, in $\sim 20\%$ of giant elliptical galaxies (e.g., van Dokkum & Franx 1995; Verdoes Kleijn et al. 1999; Capetti et al. 2000; de Koff et al. 2000; Tomita et al. 2000; Tran et al. 2001; Laine et al. 2003).

Jaffe et al. (1999) show that nuclear gas disks in early-type galaxies fall into two general categories. The most common type are dusty disks, which are easily detected by their obscuration in broad-band optical *HST* images. The dust is usually accompanied by an ionized component. Figure 1.2 shows an example, the disk in the S0 galaxy NGC 3245. The second class consists of ionized gas without associated dust disks. M87 (Ford et al. 1994) is the prototype of this category. Ionized disks are sometimes found to have filamentary or spiral structure, and patches of dust may be present as well. A comprehensive study of disk orientations in radio galaxies by Schmitt et al. (2002) finds that the radio jets are not preferentially aligned along the disk rotation axis, although jets tend not to be oriented close to the disk plane.

Soon after the first *HST* servicing mission, the first spectroscopic investigations of the kinematics of these disks were performed with the Faint Object Spectrograph (FOS). The first target was M87, for which Harms et al. (1994) detected a steep velocity gradient across the nucleus in the $H\alpha$, $[N II]$, and $[O III]$ emission lines, consistent with Keplerian rotation in an inclined disk. The central mass was found to be $(2.4 \pm 0.7) \times 10^9 M_\odot$, remarkably close to the values first determined by Young et al. (1978) and Sargent et al. (1978). The second gas-dynamical study with *HST* found a central dark mass of $(4.9 \pm 1.0) \times 10^8 M_\odot$ in the radio galaxy NGC 4261 (Ferrarese, Ford, & Jaffe 1996). These dramatic results opened a new chapter in the search for supermassive black holes, demonstrating that spatially resolved gas disks could indeed be used to measure the central masses of galaxies. In contrast to stellar dynamics, the gas-dynamical method is extremely appealing in its sim-

plicity. Modeling the kinematics of a thin, rotating disk is conceptually straightforward. Furthermore, observations of emission-line velocity fields require less telescope time than absorption-line spectroscopy. Since the FOS was a single-aperture spectrograph, however, it was not well-suited to the task of mapping out emission-line velocity fields in detail, and FOS gas-dynamics data were only obtained for a few additional galaxies (van der Marel & van den Bosch 1998; Ferrarese & Ford 1999; Verdoes Kleijn et al. 2000).

After the initial FOS detections, progress was made on two fronts. The installation of the Space Telescope Imaging Spectrograph (STIS), a long-slit instrument, greatly expanded the capabilities of *HST* for dynamical measurements. In addition, the development of techniques to model the kinematic data in detail led to more robust measurements. At the center of a disk, the large spatial gradients in rotation velocity and emission-line surface brightness are smeared out by the telescope point-spread function (PSF) and by the nonzero size of the spectroscopic aperture. Macchetto et al. (1997) and van der Marel & van den Bosch (1998) were the first to model the effects of instrumental blurring on *HST* gas-kinematic data, and detailed descriptions of modeling techniques have been given by Barth et al. (2001), Maciejewski & Binney (2001), and Marconi et al. (2003).

The feasibility of performing a black hole detection in any given galaxy can be roughly quantified in terms of r_G , the radius of the “sphere of influence” over which the black hole dominates the gravitational potential of its host galaxy. This quantity is given by $r_G = GM_\bullet/\sigma_\star^2$. Projected onto the sky, and scaled to typical parameters for an *HST* measurement, this corresponds to

$$r_G = 0.11 \left(\frac{M_\bullet}{10^8 M_\odot} \right) \left(\frac{200 \text{ km s}^{-1}}{\sigma_\star} \right)^2 \left(\frac{20 \text{ Mpc}}{D} \right) \text{ arcsec.} \quad (1.1)$$

Detection of black holes via their influence on the motions of stars or gas is most readily accomplished when observations are able to probe spatial scales smaller than r_G , but it should be borne in mind that this is at best an approximate criterion. The stellar velocity dispersion is an aperture-dependent quantity, so there is no uniquely determined value of r_G for a given galaxy. Even when r_G is unresolved the black hole will still influence the motions of stars and gas at larger radii. In stellar-dynamical measurements, it is possible to obtain information from spatial scales smaller than the instrumental resolution by measuring higher-order moments of the central line-of-sight velocity profile, since extended wings on the velocity profile are the signature of high-velocity stars orbiting close to the black hole (e.g., van der Marel 1994). With sufficiently high signal-to-noise ratio, the information contained in the full line-of-sight velocity profile could be exploited in gas-dynamical measurements as well, although measurements to date have generally been performed by fitting models to the first and second moments of the velocity distribution function (i.e., the mean velocity and line width at each observed position), or in some cases only to the mean velocities.

The analysis of a gas-dynamical dataset consists of the following basic steps. The galaxy’s stellar light profile must be measured, corrected for dust absorption if necessary, and converted to a three-dimensional luminosity density. The stellar mass density is generally assumed to be axisymmetric or spherically symmetric. A model velocity field is computed for the combined potential of the black hole and the galaxy mass distribution, usually assuming a spatially constant stellar mass-to-light ratio (M/L). After projecting the velocity field to a given distance and inclination angle, the model is synthetically “observed” by simulating

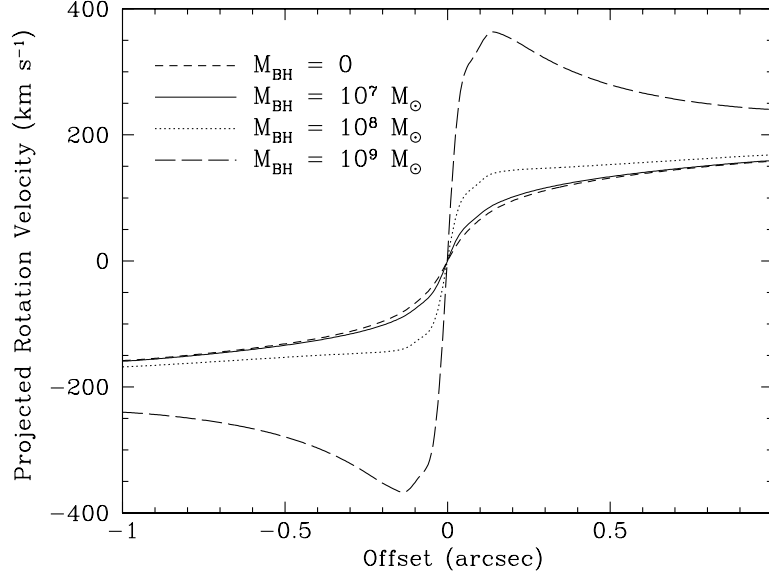


Fig. 1.3. Projected radial velocity curves for the major axis of a model disk with $i = 60^\circ$ at $D = 20$ Mpc, for $M_\bullet = 0, 10^7, 10^8$, and $10^9 M_\odot$. The models are convolved with the *HST* PSF and sampled over a slit width of $0''.1$. The curves illustrate the mean velocity observed at each position along the spectrograph slit.

the passage of light through the spectrograph optics and measuring the resulting model line profiles. Finally, the model fit to the measured emission-line velocity field is optimized to obtain the best-fitting value of M_\bullet . In addition to M_\bullet , the free parameters in the kinematic model fit include the disk inclination and major axis position angle, and the stellar M/L ; these can be determined from the kinematic data if observations are obtained at three or more parallel positions of the spectrograph slit. Maciejewski & Binney (2001) have shown that when the slit is wider than the PSF core, there is an additional signature of the black hole: at one particular location in the velocity field, the rotational and instrumental broadening will be oppositely directed, and they will very nearly cancel, giving a very narrow line profile. The location of this feature can be used as an additional diagnostic of M_\bullet . With up-to-date analysis techniques and high-quality STIS data, it is possible to achieve formal measurement uncertainties on M_\bullet of order $\sim 25\%$ or better for galaxies with well-behaved disks (e.g., Barth et al. 2001). This makes the gas-dynamical method very competitive with the precision that can be achieved by stellar-dynamical measurements.

Figure 1.3 illustrates model calculations for the projected radial velocities along the major axis of an inclined gas disk. The models have been calculated for a disk inclined at 60° to the line of sight, in a galaxy at a distance of 20 Mpc with $M_\bullet = 0, 10^7, 10^8$, and $10^9 M_\odot$. To demonstrate the effects of varying M_\bullet , the same stellar mass profile has been used for all four models. The model velocity fields have been convolved with the STIS PSF and sampled over an aperture corresponding to an $0''.1$ -wide slit, and the curves represent the mean velocity that would be observed as a function of position along the slit. At one extreme,

the sphere of influence of the $10^7 M_\odot$ black hole is unresolved, and the $10^7 M_\odot$ model is barely distinguishable from the model with no black hole, although the rapidly rotating gas near the black hole will give rise to high-velocity wings on the central emission-line profile. The opposite extreme is the $10^9 M_\odot$ black hole, for which the Keplerian region is extremely well resolved and the black hole would be readily detected. Instrumental blurring causes a turnover in the velocity curves at about $0''.15$ in this case, and Keplerian rotation can only be clearly detected at larger radii. Thus, Keplerian rotation can only be verified in detail (in the sense of having several independent data points to trace the $v \propto r^{-1/2}$ dependence) for galaxies with exceptionally well-resolved r_G . To date, the only published *HST* gas-dynamical measurements that have unambiguously detected the Keplerian region are those of M87 (Macchetto et al. 1997) and M84 (Bower et al. 1998).

The middle ground between these two extremes is illustrated by the $10^8 M_\odot$ black hole in Figure 1.3. In this case, the Keplerian rise in velocity is not detected; instead, a steep but smooth velocity gradient across the nucleus is observed. The mass of the black hole can still be determined from the steepness of this central gradient, provided that the observations give sufficient information to distinguish the velocity curves from those of the $M_\bullet = 0$ case. It is possible in principle to measure M_\bullet even in galaxies for which r_G is formally unresolved, if it can be shown that the disk has an excess rotation velocity relative to the best-fitting model without a black hole. However, in such cases there are practical complications that may limit the measurement accuracy: it is critical to determine the stellar luminosity density profile and M/L accurately, and spatial gradients in M/L are an added complication. In general, the most confident detections of black holes will be in those relatively rare objects for which the Keplerian region can be clearly traced, but the majority of gas-dynamical mass measurements will come from objects for which the mass is determined primarily from the steepness of the central velocity gradient rather than from fitting models to a well-resolved Keplerian velocity field.

Since the gas can respond to nongravitational forces, it is essential for the observations to map the disk structure in sufficient detail that the assumption of gravitational motion can be tested. This is a nontrivial concern, as there are examples of galaxies in which the gas does not rotate at the circular velocity (e.g., Fillmore, Boroson, & Dressler 1986; Kormendy & Westpfahl 1989). The case of IC 1459 serves as a cautionary tale. FOS observations at 6 positions within $0''.3$ of the nucleus revealed a steep central velocity gradient in the ionized gas, and disk model fits implied the presence of a central dark mass of $(1-4) \times 10^8 M_\odot$ (Verdoes Kleijn et al. 2000). More recently, STIS observations have mapped out the circumnuclear kinematics in much greater detail and found an irregular and asymmetric velocity field that cannot be interpreted in terms of flat disk models; a stellar-dynamical analysis finds $M_\bullet = (2.6 \pm 1.1) \times 10^9 M_\odot$ (Cappellari et al. 2002). Thus, the ionized gas fails to be a useful probe of the gravitational potential in this galaxy.

Most of the nuclear disks observed spectroscopically with *HST* have revealed evidence for substantial internal velocity dispersions, even when the velocity field is clearly dominated by rotation. That is, the gas disks are not in purely quiescent circular rotation, and the disks have some degree of internal velocity structure or turbulence. The intrinsic emission-line velocity dispersion σ_{gas} tends to be greatest at the nucleus, and observed values span a wide range, exceeding 500 km s^{-1} in extreme cases (e.g., van der Marel & van den Bosch 1998).

The origin of this internal velocity dispersion is unknown, and the interpretation of σ_{gas} remains the single most important unresolved problem for gas-dynamical measurements of

black hole masses. In a study of the radio galaxy NGC 7052, van der Marel & van den Bosch (1998) argued that σ_{gas} was due to local turbulence in gas that remained in bulk motion on circular orbits at the local circular velocity. Another possibility that has been considered is that the disks are composed of a large number of clouds with small filling factor, and that the individual clouds are on noncircular orbits that are nevertheless dominated by gravity (e.g., Verdoes Kleijn et al. 2000). This is analogous to the effect of “asymmetric drift” that is well known in stellar dynamics (e.g., Binney & Tremaine 1987). In this situation, the gas disk would be supported against gravity by both rotation and random motions, and models based on pure circular rotation would underestimate the true black hole masses. The asymmetric drift correction to M_{\bullet} is expected to be small when $(\sigma_{\text{gas}}/v_{\text{rot}})^2 \ll 1$, but this must be tested on a case-by-case basis by computing models for the emission-line widths. Various approaches to calculating the asymmetric drift in gas disks have been presented by Cretton, Rix, & de Zeeuw (2000), Verdoes Kleijn et al. (2000, 2002), and Barth et al. (2001).

Since different groups have used a variety of methods to treat this problem in dynamical analyses (sometimes ignoring it altogether), and since σ_{gas} varies widely among different galaxies, the influence of the intrinsic velocity dispersion could be responsible for some of the apparent scatter in the $M_{\bullet} - \sigma_{\star}$ relation. Now that large samples of galaxies have been observed with STIS, it may be possible to discern whether there are any correlations of σ_{gas} with the level of nuclear activity or with the Hubble type or any other property of the host galaxy; detection of any clear trends might help to elucidate the origin of the intrinsic dispersion. Three-dimensional hydrodynamical simulations have evolved to the point where it is now becoming feasible to model the turbulent structure of gas disks in galaxies (e.g., Wada, Meurer, & Norman 2002); this work may lead to new insights on how best to interpret σ_{gas} in gas-dynamical measurements. Further discussion of the intrinsic velocity dispersion problem is presented by Verdoes Kleijn, van der Marel, & Noel-Storr (2003).

Most gas-dynamical studies to date have concentrated on elliptical and S0 galaxies, but STIS data have now been obtained for dozens of spiral galaxies as well (e.g., Marconi et al. 2003). In principle, the gas-dynamical method can work equally well for spirals, but there are some additional complications. One is the presence of nuclear star clusters, which are nearly ubiquitous in late-type spirals (Carollo, Stiavelli, & Mack 1998; Böker et al. 2002). The nuclear star clusters are typically young (Walcher et al. 2003), and the dynamical modeling must take into account the possible radial gradient in M/L . Another caveat is that spiral arms or bar structure can lead to departures from circular rotation in the ionized gas (Koda & Wada 2002; Maciejewski 2003). Only $\sim 10\% - 20\%$ of spirals appear to have orderly emission-line velocity fields suitable for disk-model fitting to derive M_{\bullet} (Sarzi et al. 2001), so some care is needed when selecting targets for *HST* gas-dynamical surveys. Ho et al. (2002) have shown that orderly rotation in the emission-line gas almost exclusively occurs in galaxies having orderly, symmetric circumnuclear dust-lane morphology that can be detected in *HST* imaging data, and this offers a promising way to maximize the rate of successful M_{\bullet} measurements in future programs.

Even when gas-dynamical data cannot provide a direct measurement of black hole mass, either due to insufficient resolution or irregular kinematics, they can still be used to derive upper limits to M_{\bullet} from the central amplitude of the rotation curve or the central emission-line width. For galaxies with $\sigma_{\star} \lesssim 100 \text{ km s}^{-1}$, where direct measurements of M_{\bullet} are scarce, upper limits are valuable additions to the black hole census. For example, from a large sample of ground-based rotation curves, Salucci et al. (2000) demonstrated that late-type

spirals must generally have $M_{\bullet} \lesssim 10^{6-7} M_{\odot}$. Sarzi et al. (2002) measured upper limits to M_{\bullet} from the central emission-line widths observed in STIS spectra of 16 galaxies having σ_{\star} between 80 and 270 km s⁻¹. The derived upper limits are consistent with the $M_{\bullet} - \sigma_{\star}$ relation, further confirming that few galaxies (perhaps none) are strong outliers with very overmassive black holes relative to their bulge luminosity or velocity dispersion.

Gas-dynamical measurements using *HST* data have now been published for about a dozen galaxies (Harms et al. 1994; Ferrarese et al. 1996; Macchetto et al. 1997; Bower et al. 1998; van der Marel & van den Bosch 1998; Ferrarese & Ford 1999; Barth et al. 2001; Sarzi et al. 2001; Verdoes Kleijn et al. 2002; Marconi et al. 2003). The results, together with stellar-dynamical measurements, have been compiled by Kormendy & Gebhardt (2001), Merritt & Ferrarese (2001), and Tremaine et al. (2002). This number will continue to increase over the next several years, since STIS gas-kinematic observations have been obtained or scheduled for over 100 galaxies. However, it remains to be seen how many of these datasets will lead to accurate measurements of black hole masses. A substantial fraction of the galaxies will probably not have well-behaved gas disks suitable for modeling, and in many of the target galaxies r_G may be much smaller than the resolution limit of *HST* (Merritt & Ferrarese 2002). Thus, it remains worthwhile to search for additional nearby galaxies having morphologically regular disks that will make promising targets for future spectroscopic observations.

With the small projected sizes of r_G in most nearby galaxies, ground-based observations cannot generally be used to perform gas-dynamical measurements of M_{\bullet} . One exception is the nearby ($D = 3.5$ Mpc) radio galaxy Cen A. Marconi et al. (2001) obtained near-infrared spectra of this galaxy in 0.''5 seeing, and measured the velocity field of the Pa β and [Fe II] emission lines. They detected a steep central velocity gradient with a turnover to Keplerian rotation outside the region dominated by atmospheric seeing, and derived a central dark mass of $2^{+3.0}_{-1.4} \times 10^8 M_{\odot}$. Although the black hole mass was not determined with very high precision, this measurement serves as a proof of concept that ground-based observations of near-infrared emission lines can be used for gas-dynamical analysis. With future laser guide star systems, such measurements can be performed using adaptive optics on 8–10 meter telescopes, although the possibility of a spatially and temporally variable PSF will make the data analysis a formidable challenge. Also, the *Atacama Large Millimeter Array* will provide new high-resolution views of circumnuclear disks and new probes of disk dynamics with molecular emission lines.

1.3 Black Hole Masses from Observations of H₂O Masers

Water vapor maser emission at $\lambda = 1.35$ cm from the nucleus of the low-luminosity Seyfert 2 galaxy NGC 4258 was detected by Claussen, Heiligman, & Lo (1984). The maser emission consists of a bright core with several distinct components near the systemic velocity arranged in an elongated region (Greenhill et al. 1995), as well as “satellite” lines separated by $\pm 800 - 1000$ km s⁻¹ from the systemic features (Nakai, Inoue, & Miyoshi 1993). The presence of high-velocity emission was suggestive of a disk rotating about a central mass of $\sim 10^7 M_{\odot}$ (Watson & Wallin 1994), and the breakthrough observation came when Miyoshi et al. (1995) used the Very Long Baseline Array to map out the positions of the high-velocity features. They found that the satellite masers traced out a near-perfect Keplerian velocity curve on either side of the nucleus, allowing a precise determination of the enclosed mass within the inner radius of the disk (3.9 milliarcsec, corresponding to a radius of only 0.14

pc). For a distance of 7.2 Mpc, the central mass is found to be $3.9 \times 10^7 M_{\odot}$. It is very unlikely that this mass could be composed of a cluster of dark objects such as stellar remnants or brown dwarfs, since the cluster density would be so large that its lifetime against evaporation or collisions would be short compared to the age of the galaxy (Maoz 1995, 1998). This makes NGC 4258 the most compelling dynamical case for the existence of a supermassive black hole outside of our own Galaxy. Recently, a preliminary analysis of *HST* stellar-dynamical data for NGC 4258 has yielded a value of M_{\bullet} consistent with the maser measurement (Siopis et al. 2002); this is a reassuring confirmation of the stellar-dynamical technique.

A detailed review of the properties of the NGC 4258 maser system and a listing of other known H₂O maser galaxies is given by Moran, Greenhill, & Herrnstein (1999). Hundreds of galaxies have been surveyed for H₂O masers (e.g., Braatz, Wilson, & Henkel 1996; Greenhill et al. 2002, 2003), and there are about 30 known sources to date. Braatz et al. (1997) find that powerful H₂O masers are only detected in Seyfert 2 and LINER nuclei, and not in Seyfert 1 galaxies. This is consistent with the geometrical picture of AGN unification models, which posit the existence of an edge-on torus or disk in the Type 2 objects. The large path length along our line of sight in an edge-on disk permits maser amplification, while a more face-on disk in a Type 1 AGN would not emit maser lines in our direction. Further confirmation of this geometric structure comes from detection of large X-ray obscuring columns (e.g., Makishima et al. 1994; Iwasawa, Maloney, & Fabian 2002) and polarized emission lines from obscured nuclei (e.g., Antonucci & Miller 1985; Wilkes et al. 1995) in some H₂O maser galaxies.

Disklike structures have been detected in several other maser galaxies, but NGC 4258 remains the only one for which the central mass has been derived with high precision. The maser clouds in NGC 1068 appear to trace the surface of a geometrically thick torus rather than a thin disk, and their velocities fall below a Keplerian curve, suggesting a central mass of $\sim 10^7 M_{\odot}$ (Greenhill et al. 1996). NGC 4945 contains high-velocity maser clumps in a roughly disklike arrangement, but with larger uncertainties than for NGC 4258; the central mass is $\sim 10^6 M_{\odot}$ within a radius of 0.3 pc (Greenhill, Moran, & Herrnstein 1997). Recently, high-velocity maser features have been detected in IC 2560 (Ishihara et al. 2001), NGC 5793 (Hagiwara et al. 2001), NGC 2960 (Henkel et al. 2002), and the Circinus galaxy (Greenhill et al. 2003), and VLBI measurements can determine whether the masers in these galaxies trace out Keplerian rotation curves. Additional maser disks will continue to be found in future surveys, although the nearby AGN population has now been surveyed so thoroughly that it is unlikely that many more new examples will be found at distances comparable to that of NGC 4258.

1.4 Reverberation Mapping

Reverberation mapping uses temporal variability of active nuclei to probe the size and structure of the broad-line region (BLR) of Seyfert 1 galaxies and quasars. The basic principle is that variability in the ionizing photon output of the central engine will be followed by corresponding variations in the emission-line luminosity, after a time delay dependent on the light-travel time between the ionizing source and the emission-line clouds (Blandford & McKee 1982). By monitoring the continuum and emission-line brightness of a broad-lined AGN over a sufficient time period, the lag between continuum variations and emission-line response can be derived, giving a size scale for the region emitting the line;

typical sizes range from a few light-days up to ~ 1 light-year. Thus, the method makes use of the time domain to resolve structures that cannot be resolved spatially, and the measurement accuracy depends on temporal sampling rather than spatial resolution. Peterson (2001) gives a thorough discussion of the observational and analysis techniques used in reverberation-mapping campaigns. The literature on reverberation mapping is extensive, and this section reviews only a few recent results on the determination of black hole masses from reverberation data.

If the motions in the BLR are dominated by gravity (rather than, for example, radiatively driven outflows), then the central mass can be derived from the BLR radius combined with a characteristic velocity. Essentially, the black hole mass is derived as $M_{\bullet} = f v^2 r / G$, where v is some measure of the broad-line velocity width (typically the full width at half maximum), r is the BLR radius derived from the measured time delay, and f is an order-unity factor that depends on the geometry of the BLR (i.e., disklike or spherical). Reverberation masses for 34 Seyfert 1 galaxies and low-redshift quasars have been determined by Wandel, Peterson, & Malkan (1999) and Kaspi et al. (2000). The method is subject to some potentially serious systematic errors, however, as emphasized by Krolik (2001); the unknown geometry and emissivity distribution of the BLR clouds can lead to biases in the derived masses, and it is critically important to verify that the BLR velocity field is in fact dominated by gravitational motion.

Recent observations have yielded some encouraging results. Since the BLR is radially stratified in ionization level, highly ionized clouds emitting He II and C IV respond most quickly to continuum variations, with response times of a few days, while lines such as H β and C III] $\lambda 1909$ have longer lag times as well as narrower widths. Thus, if lag times t_{lag} can be measured for multiple broad emission lines in a given galaxy, it is possible to trace out the velocity structure of the BLR as a function of radius. Peterson & Wandel (1999, 2000) and Onken & Peterson (2002) have shown that for four of the best-observed reverberation targets, NGC 3783, NGC 5548, NGC 7469, and 3C 390.3, the relation between t_{lag} and emission-line width shows exactly the dependence expected for Keplerian motion. Within the measurement uncertainties, the emission lines in each galaxy yield a correlation consistent with $\text{FWHM} \propto t_{\text{lag}}^{0.5}$, and for each galaxy the time lags and line widths of the different emission lines give consistent results for the central mass.

Another key question is whether reverberation mapping yields black hole masses that are consistent with the host galaxy properties of the AGNs. Gebhardt et al. (2000b) and Ferrarese et al. (2001) demonstrated that the reverberation masses and velocity dispersions of several Seyfert nuclei are in good agreement with the $M_{\bullet} - \sigma_{\star}$ relation of inactive galaxies. Nelson (2000) performed a similar analysis for a larger sample, using [O III] line widths as a substitute for σ_{\star} , and found similar results, albeit with additional scatter that could be attributed to some nongravitational motion in the narrow-line region. Some previous studies had found the puzzling result that the AGNs seemed to have systematically lower $M_{\bullet}/M_{\text{bulge}}$ ratios than inactive galaxies (Ho 1999; Wandel 1999). Since the AGNs do not appear discrepant in the $M_{\bullet} - \sigma_{\star}$ relation, a likely conclusion (e.g., Wandel 2002) is that the bulge luminosities of the Seyferts had been systematically overestimated, due to a combination of their relatively large distances and the dominance of the central point sources; starburst activity in the Seyferts might further bias the photometric decompositions toward anomalously high bulge luminosities.

Overall, the agreement between the $M_{\bullet} - \sigma_{\star}$ relation of Seyferts with that of inactive

galaxies suggests that the reverberation masses are probably accurate to a factor of ~ 3 on average (Peterson 2003). Direct measurements of M_\bullet in reverberation-mapped Seyferts with *HST* would be a valuable cross-check, but unfortunately only a few bright Seyfert 1 galaxies are near enough for r_G to be resolved, and attempts to perform stellar-dynamical measurements of the nearest objects with *HST* have been thwarted by the dominance of the bright nonstellar continuum. Gas-dynamical observations are not affected by this problem, and there have been attempts to detect cleanly rotating kinematic components in Seyfert narrow-line regions that could be used for M_\bullet measurements with *HST* (Winge et al. 1999). Unfortunately, the presence of outflows or other kinematic disturbances typically precludes the use of emission-line velocity fields as probes of M_\bullet in Seyfert 1 galaxies (e.g., Crenshaw et al. 2000). Since there is no way to perform direct stellar- or gas-dynamical measurements of M_\bullet in most reverberation-mapped AGNs, the comparison with the $M_\bullet - \sigma_*$ relation remains the main consistency check that can currently be applied to the reverberation-based masses.

Reverberation mapping can be extended to higher redshifts, since it is not dependent on spatial resolution, but the longer variability time scales for higher-mass black holes in luminous quasars, combined with cosmological time dilation, can require monitoring campaigns with durations that are a significant fraction of an individual astronomer's career! Kaspi et al. (2003) present preliminary results from an ongoing, eight-year campaign to monitor 11 luminous quasars at $2.1 < z < 3.2$. Continuum variations have been detected, but the corresponding emission-line variability has not yet been seen. Reverberation observations of quasars are a fundamental probe of black hole masses at high redshift, and efforts to monitor additional quasars over a wide redshift range should be encouraged, despite the long time scales involved.

One important consequence of the reverberation campaigns has been the detection of a correlation between the BLR radius and the continuum luminosity, a result that is expected on the basis of simple photoionization considerations (e.g., Wandel 1997). With a sample of 34 reverberation-mapped AGNs, Kaspi et al. (2000) find $r_{\text{BLR}} \propto L^{0.7}$ using continuum luminosity at 5100 Å. This correlation offers an extremely valuable shortcut to estimate the BLR size, and black hole mass, in distant quasars. While reverberation campaigns require years of intensive observations, $L(5100 \text{ Å})$ and $\text{FWHM}(\text{H}\beta)$ can be measured from a single spectrum, and then combined to yield an estimate of M_\bullet under the assumption of virial motion of the BLR clouds. This is the only technique that can routinely be applied to derive M_\bullet in distant AGNs, and it has recently been the subject of intense interest, with numerous studies focused on topics such as the $M_\bullet/M_{\text{bulge}}$ ratio in quasars and the search for possible differences between radio-loud and radio-quiet objects (e.g., Laor 1998, 2001; Lacy et al. 2001; McLure & Dunlop 2001, 2002; Jarvis & McLure 2002; Oshlack, Webster, & Whiting 2002; Shields et al. 2003). The technique has also been extended to make use of continuum luminosity in the rest-frame ultraviolet combined with the velocity width of either C IV (Vestergaard 2002) or Mg II (McLure & Jarvis 2002), so that ground-based, optical spectra can be used to derive black hole masses for high-redshift quasars.

These secondary methods are extremely valuable since they offer the most straightforward estimates of black hole masses at high redshift, although there are potential biases that must be kept in mind. The derived BLR size and M_\bullet depend on the observed continuum luminosity, but this can be affected by dust extinction (Baker & Hunstead 1995) or by relativistic beaming of synchrotron emission in radio-loud objects (Whiting, Webster, & Francis 2001). If the BLR has a flattened, disklike geometry, then the effects of source orienta-

tion on the observed line width must be accounted for (e.g., McLure & Dunlop 2002). An additional concern is that the $r_{\text{BLR}}-L$ relation has only been calibrated against the Kaspi et al. reverberation sample, which covers a somewhat limited range both in black hole mass ($M_{\bullet} \lesssim 5 \times 10^8 M_{\odot}$) and in luminosity ($\lambda L_{\lambda} \lesssim 7 \times 10^{45} \text{ erg s}^{-1}$ at 5100 Å). Application of this method to high-luminosity quasars with $M_{\bullet} > 10^9 M_{\odot}$ necessarily involves a large extrapolation (see Netzer 2003 for further discussion). These issues can be overcome if reverberation masses can be derived for larger samples of quasars, extending to high intrinsic luminosities and $M_{\bullet} > 10^9 M_{\odot}$, so that the relations between M_{\bullet} , line width, and luminosity can be calibrated over a broader parameter space.

1.5 Future Work and Some Open Questions

I conclude with a very incomplete list of a few important and tractable problems that can be addressed in the foreseeable future by new observations.

1. More dynamical measurements of black hole masses in nearby galaxies are needed, over the widest possible range of host galaxy masses and velocity dispersions, so that the slope of the $M_{\bullet}-\sigma_{\star}$ and $M_{\bullet}-L_{\text{bulge}}$ correlations can be determined definitively. To constrain the amount of intrinsic scatter in these correlations, realistic estimates of the measurement uncertainties are crucial. Gas-dynamical measurements with *HST* and, in the future, from ground-based telescopes with adaptive optics, will be a key component of this pursuit. Additional measurements of black hole masses from maser dynamics will be extremely valuable as well, if more galaxies with Keplerian maser disks can be found.

2. Direct comparisons of stellar- and gas-dynamical measurements for the same galaxies are a needed consistency check that should be performed for galaxies over a wide range of Hubble types and velocity dispersions.

3. What causes the intrinsic velocity dispersion observed in nuclear gas disks? Is it possible to determine central masses accurately for disks having $(\sigma_{\text{gas}}/v_{\text{rot}})^2 \approx 1$? Again, direct comparisons with stellar-dynamical observations would be very useful.

4. What can we learn about black hole demographics from AGNs at the extremes of the Hubble sequence? The broad-line widths and continuum luminosities of high-redshift quasars imply masses of up to $\sim 10^{10} M_{\odot}$ for some objects (e.g., Shields et al. 2003), but these measurements involve extrapolating the known correlation between r_{BLR} and L far beyond the mass and luminosity ranges over which it has been calibrated locally. At the other extreme, is there a lower limit to L_{bulge} or σ_{\star} below which galaxies have no central black hole at all? Dynamical searches for black holes in the nuclei of dwarf ellipticals or very late-type spirals become extremely difficult for distances beyond the Local Group (see van der Marel, this volume). On the other hand, searches for accretion-powered nuclear activity in dwarf galaxies can offer some constraints on the population of black holes with $M < 10^6 M_{\odot}$. The case of NGC 4395, a dwarf Magellanic spiral hosting a full-fledged Seyfert 1 nucleus (Filippenko & Sargent 1989) with a black hole of $\lesssim 10^5 M_{\odot}$ (Iwasawa et al. 2000; Filippenko & Ho 2003), demonstrates that at least some dwarf galaxies can host black holes that would be undetectable by dynamical means.

5. How do the $M_{\bullet}-\sigma_{\star}$ and $M_{\bullet}-L_{\text{bulge}}$ correlations evolve with redshift, and how early did the black holes in the highest-redshift quasars build up most of their mass? Reverberation mapping of high-redshift quasars, and further calibration and testing of the r_{BLR} -luminosity relationship in luminous quasars, will be of fundamental importance in answering these questions. Measurement of the masses of black holes at high redshift, as well as the lumi-

A. J. Barth

nosities and/or velocity dispersions of their host galaxies, will be a major observational step toward understanding the coevolution of black holes and their host galaxies.

References

- Antonucci, R. R. J., & Miller, J. S. 1985, *ApJ*, 297, 621
Baker, J. C., & Hunstead, R. W. 1995, *ApJ*, 452, L95
Barth, A. J., Sarzi, M., Rix, H.-W., Ho, L. C., Filippenko, A. V., & Sargent, W. L. W. 2001, *ApJ*, 555, 685
Binney, J., & Tremaine, S. 1987, *Galactic Dynamics* (Princeton: Princeton Univ. Press)
Blandford, R. D., & McKee, C. F. 1982, *ApJ*, 255, 419
Böker, T., Laine, S., van der Marel, R. P., Sarzi, M., Rix, H.-W., Ho, L. C., & Shields, J. C. 2002, *AJ*, 123, 1389
Bower, G. A., et al. 1998, *ApJ*, 492, L111
Braatz, J. A., Wilson, A. S., & Henkel, C. 1996, *ApJS*, 106, 51
———. 1997, *ApJS*, 110, 321
Capetti, A., de Ruiter, H. R., Fanti, R., Morganti, R., Parma, P., & Ulrich, M.-H. 2000, *A&A*, 362, 871
Cappellari, M., Verolme, E. K., van der Marel, R. P., Verdoes Kleijn, G. A., Illingworth, G. D., Franx, M., Carollo, C. M., & de Zeeuw, P. T. 2002, *ApJ*, 578, 787
Carollo, C. M., Stiavelli, M., & Mack, J. 1998, *AJ*, 116, 68
Chokshi, A., & Turner, E. L. 1992, *MNRAS*, 259, 421
Claussen, M. J., Heiligman, G. M., & Lo, K.-Y. 1984, *Nature*, 310, 298
Crenshaw, D. M., et al. 2000, *AJ*, 120, 1731
Cretton, N., Rix, H.-W., & de Zeeuw, P. T. 2000, *ApJ*, 536, 319
de Koff, S., et al. 2000, *ApJS*, 129, 33
Ebner, K., Davis, M., & Djorgovski, S. 1988, *AJ*, 95, 422
Ferrarese, L., & Ford, H. C. 1999, *ApJ*, 515, 583
Ferrarese, L., Ford, H. C., & Jaffe, W. 1996, *ApJ*, 470, 444
Ferrarese, L., & Merritt, D. 2000, *ApJ*, 539, L9
Ferrarese, L., Pogge, R. W., Peterson, B. M., Merritt, D., Wandel, A., & Joseph, C. L. 2001, *ApJ*, 555, L79
Filippenko, A. V., & Ho, L. C. 2003, *ApJ*, 588, L13
Filippenko, A. V., & Sargent, W. L. W. 1989, *ApJ*, 342, L11
Fillmore, J. A., Boroson, T. A., & Dressler, A. 1986, *ApJ*, 302, 208
Ford, H. C., et al. 1994, *ApJ*, 435, L27
Gebhardt, K., et al. 2000a, *ApJ*, 539, L13
———. 2000b, *ApJ*, 543, L5
Greenhill, L. J., et al. 2002, *ApJ*, 565, 836
Greenhill, L. J., Gwinn, C. R., Antonucci, R., & Barvainis, R. 1996, *ApJ*, 472, L21
Greenhill, L. J., Jiang, D. R., Moran, J. M., Reid, M. J., Lo, K.-Y., & Claussen, M. J. 1995, *ApJ*, 440, 619
Greenhill, L. J., Kondratko, P. T., Lovell, J. E. J., Kuiper, T. B. H., Moran, J. M., Jauncey, D. L., & Baines, G. P. 2003, *ApJ*, 582, L11
Greenhill, L. J., Moran, J. M., & Herrnstein, J. R. 1997, *ApJ*, 481, L23
Hagiwara, Y., Diamond, P. J., Nakai, N., & Kawabe, R. 2001, *ApJ*, 560, 119
Harms, R. J., et al. 1994, *ApJ*, 435, L35
Henkel, C., Braatz, J. A., Greenhill, L. J., & Wilson, A. S. 2002, *A&A*, 394, L23
Ho, L. C. 1999, in *Observational Evidence for Black Holes in the Universe*, ed. S. K. Chakrabarti (Dordrecht: Kluwer), 157
Ho, L. C., Sarzi, M., Rix, H.-W., Shields, J. C., Rudnick, G., Filippenko, A. V., & Barth, A. J. 2002, *PASP*, 114, 137
Ishihara, Y., Nakai, N., Iyamoto, N., Makishima, K., Diamond, P., & Hall, P. 2001, *PASJ*, 53, 215
Iwasawa, K., et al. 1996, *MNRAS*, 282, 1038
Iwasawa, K., Fabian, A. C., Almaini, O., Lira, P., Lawrence, A., Hayashida, K., & Inoue, H. 2000, *MNRAS*, 318, 879
Iwasawa, K., Maloney, P. R., & Fabian, A. C. 2002, *MNRAS*, 336, L71
Jaffe, W., Ford, H. C., Ferrarese, L., van den Bosch, F., & O'Connell, R. W. 1993, *Nature*, 364, 213
Jaffe, W., Ford, H. C., Tsvetanov, Z., Ferrarese, L., & Dressel, L. 1999, in *Galaxy Dynamics*, ed. D. Merritt, J. A. Sellwood, & M. Valluri (San Francisco: ASP), 13

A. J. Barth

- Jarvis, M. J., & McLure, R. J. 2002, *MNRAS*, 336, L38
- Kaspi, S., Netzer, H., Maoz, D., Shemmer, O., Brandt, W. N., & Schneider, D. P. 2003, in *Carnegie Observatories Astrophysics Series, Vol. 1: Coevolution of Black Holes and Galaxies*, ed. L. C. Ho (Pasadena: Carnegie Observatories, <http://www.ociw.edu/ociw/symposia/series/symposium1/proceedings.html>)
- Kaspi, S., Smith, P. S., Netzer, H., Maoz, D., Jannuzi, B. T., & Givon, U. 2000, *ApJ*, 533, 631
- Koda, J., & Wada, K. 2002, *A&A*, 396, 867
- Kormendy, J., & Gebhardt, K. 2001, in *The 20th Texas Symposium on Relativistic Astrophysics*, ed. H. Martel & J. C. Wheeler (Melville: AIP), 363
- Kormendy, J., & Richstone, D. 1995, *ARA&A*, 33, 581
- Kormendy, J., & Westpfahl, D. J. 1989, *ApJ*, 338, 752
- Kotanyi, C. G., & Ekers, R. D. 1979, *A&A*, 73, L1
- Krolik, J. H. 2001, *ApJ*, 551, 72
- Lacy, M., Laurent-Muehleisen, S. A., Ridgway, S. E., Becker, R. H., & White, R. L. 2001, *ApJ*, 551, L17
- Laine, S., van der Marel, R. P., Lauer, T. R., Postman, M., O'Dea, C. P., & Owen, F. N. 2003, *AJ*, 125, 478
- Laor, A. 1998, *ApJ*, 505, L83
- . 2001, *ApJ*, 553, 677
- Macchetto, F., Marconi, A., Axon, D. J., Capetti, A., Sparks, W., & Crane, P. 1997, *ApJ*, 489, 579
- Maciejewski, W. 2003, in *Carnegie Observatories Astrophysics Series, Vol. 1: Coevolution of Black Holes and Galaxies*, ed. L. C. Ho (Pasadena: Carnegie Observatories, <http://www.ociw.edu/ociw/symposia/series/symposium1/proceedings.html>)
- Maciejewski, W., & Binney, J. 2001, *MNRAS*, 323, 831
- Makishima, K., et al. 1994, *PASJ*, 46, L77
- Maoz, E. 1995, *ApJ*, 447, L91
- . 1998, *ApJ*, 494, L181
- Marconi, A., et al. 2003, *ApJ*, 586, 868
- Marconi, A., Capetti, A., Axon, D. J., Koekemoer, A., Macchetto, D., & Schreier, E. J. 2001, *ApJ*, 549, 915
- McLure, R. J., & Dunlop, J. S. 2001, *MNRAS*, 327, 199
- . 2002, *MNRAS*, 331, 795
- McLure, R. J., & Jarvis, M. J. 2002, *MNRAS*, 337, 109
- Merritt, D., & Ferrarese, L. 2001, in *The Central Kpc of Starbursts and AGN: The La Palma Connection*, ed. J. H. Knapen et al. (San Francisco: ASP), 335
- Miyoshi, M., Moran, J., Herrnstein, J., Greenhill, L., Nakai, N., Diamond, P., & Inoue, M. 1995, *Nature*, 373, 127
- Moran, J. M., Greenhill, L. J., & Herrnstein, J. R. 1999, *Jour. Astrophys. and Astron.*, 20, 165
- Nakai, N., Inoue, M., & Miyoshi, M. 1993, *Nature*, 361, 6407
- Nandra, K., George, I. M., Mushotzky, R. F., Turner, T. J., & Yaqoob, T. 1997, *ApJ*, 477, 602
- Nelson, C. H. 2000, *ApJ*, 544, L91, 199
- Netzer, H. 2003, *ApJ*, 583, L5
- Onken, C. A., & Peterson, B. M. 2002, *ApJ*, 572, 746
- Oshlack, A. Y. K. N., Webster, R. L., & Whiting, M. T. 2002, *ApJ*, 576, 81
- Peterson, B. M. 2001, in *Advanced Lectures on the Starburst-AGN Connection*, ed. I. Aretxaga, D. Kunth, & R. Mújica (Singapore: World Scientific), 3
- . 2003, in *Active Galactic Nuclei: from Central Engine to Host Galaxy*, ed. S. Collin, F. Combes, & I. Shlosman (San Francisco: ASP), in press
- Peterson, B. M., & Wandel, A. 1999, *ApJ*, 521, L95
- . 2000, *ApJ*, 540, L13
- Rees, M. J. 1984, *ARA&A*, 22, 471
- Sadler, E. M., & Gerhard, O. E. 1985, *MNRAS*, 214, 177
- Salpeter, E. E. 1964, *ApJ*, 140, 796
- Salucci, P., Ratnam, C., Monaco, P., & Danese, L. 2000, *MNRAS*, 317, 488
- Sargent, W. L. W., Young, P. J., Boksenberg, A., Shortridge, K., Lynds, C. R., & Hartwick, F. D. A. 1978, *ApJ*, 221, 731
- Sarzi, M., et al. 2002, *ApJ*, 567, 237
- Sarzi, M., Rix, H.-W., Shields, J. C., Rudnick, G., Ho, L. C., McIntosh, D. H., Filippenko, A. V., & Sargent, W. L. W. 2001, *ApJ*, 550, 65
- Schmitt, H. R., Pringle, J. E., Clarke, C. J., & Kinney, A. L. 2002, *ApJ*, 575, 150
- Shields, G. A., Gebhardt, K., Salvander, S., Wills, B., Xie, B., Brotherton, M. S., Yuan, J., Dietrich, M. 2002, *ApJ*, 583, 124

A. J. Barth

- Siopis, C., et al. 2002, BAAS, 201, 6802
- Small, T. A., & Blandford, R. D. 1992, MNRAS, 259, 725
- Softan, A. 1982, MNRAS, 200, 115
- Tanaka, Y., et al. 1995, Nature, 375, 659
- Tomita, A., Aoki, K., Watanabe, M., Takata, T., & Ichikawa, S. 2000, AJ, 120, 123
- Tran, H. D., Tsvetanov, Z., Ford, H. C., Davies, J., Jaffe, W., van den Bosch, F. C., & Rest, A. 2001, AJ, 121, 2928
- Tremaine, S., et al. 2002, ApJ, 574, 740
- van der Marel, R. P. 1994, ApJ, 432, L91
- van der Marel, R. P., & van den Bosch, F. C. 1998, AJ, 116, 2220
- van Dokkum, P. G., & Franx, M. 1995, AJ, 110, 2027
- Verdoes Kleijn, G. A., Baum, S. A., de Zeeuw, P. T., & O'Dea, C. P. 1999, AJ, 118, 2592
- Verdoes Kleijn, G. A., van der Marel, R. P., Carollo, C. M., & de Zeeuw, P. T. 2000, AJ, 120, 1221
- Verdoes Kleijn, G. A., van der Marel, R. P., de Zeeuw, P. T., Noel-Storr, J., & Baum, S. A. 2002, AJ, 124, 2524
- Verdoes Kleijn, G. A., van der Marel, R. P., & Noel-Storr, J. 2003, in Carnegie Observatories Astrophysics Series, Vol. 1: Coevolution of Black Holes and Galaxies, ed. L. C. Ho (Pasadena: Carnegie Observatories, <http://www.ociw.edu/ociw/symposia/series/symposium1/proceedings.html>)
- Vestergaard, M. 2002, ApJ, 571, 733
- Wada, K., Meurer, G., & Norman, C. A. 2002, ApJ, 577, 197
- Walcher, C. J., Häring, N., Böker, T., Rix, H.-W., van der Marel, R. P., Gerssen, J., Ho, L. C., & Shields, J. C. 2003, in Carnegie Observatories Astrophysics Series, Vol. 1: Coevolution of Black Holes and Galaxies, ed. L. C. Ho (Pasadena: Carnegie Observatories, <http://www.ociw.edu/ociw/symposia/series/symposium1/proceedings.html>)
- Wandel, A. 1997, ApJ, 490, L131
- . 1999, ApJ, 519, L39
- . 2002, ApJ, 565, 762
- Wandel, A., Peterson, B. M., & Malkan, M. A. 1999, ApJ, 526, 579
- Watson, W. D. & Wallin, B. K. 1994, ApJ, 432, L35
- Whiting, M. T., Webster, R. L., & Francis, P. J. 2001, MNRAS, 323, 718
- Wilkes, B. J., Schmidt, G. D., Smith, P. S., Mathur, S., & McLeod, K. K. 1995, ApJ, 455, L13
- Winge, C., Axon, D. J., Macchetto, F. D., Capetti, A., & Marconi, A. 1999, ApJ, 519, 134
- Young, P. J., Westphal, J. A., Kristian, J., Wilson, C. P., & Landauer, F. P. 1978, ApJ, 221, 721
- Zel'dovich, Ya. B., & Novikov, I. D. 1964, Sov. Phys. Dokl., 158, 811